Infrared Emission Spectra and Equilibrium Structures of Gaseous HgH$_2$ and HgD$_2$

Alireza Shayesteh, Shanshan Yu, and Peter F. Bernath*

Department of Chemistry, University of Waterloo, Waterloo, ON, N2L 3G1, Canada

Received: July 20, 2005; In Final Form: September 15, 2005

A detailed analysis of the high-resolution infrared emission spectra of gaseous HgH$_2$ and HgD$_2$ in the 1200−2200 cm^{-1} spectral range is presented. The ν_3 antisymmetric stretching fundamental bands of ^{204}HgH$_2$, ^{202}HgH$_2$, ^{201}HgH$_2$, ^{200}HgH$_2$, ^{199}HgH$_2$, ^{198}HgH$_2$, ^{204}HgD$_2$, ^{202}HgD$_2$, ^{201}HgD$_2$, ^{200}HgD$_2$, ^{199}HgD$_2$, and ^{198}HgD$_2$, as well as a few hot bands involving ν_1, ν_2, and ν_3 were analyzed rotationally, and spectroscopic constants were obtained. Using the rotational constants of the 000, 100, 01^{1}0, and 001 vibrational levels, we determined the equilibrium rotational constants (B_e) of the most abundant isotopologues, ^{202}HgH$_2$ and ^{202}HgD$_2$, to be 3.135325(24) cm^{-1} and 1.569037(16) cm^{-1}, respectively, and the associated equilibrium Hg−H and Hg−D internuclear distances (r_e) are 1.63324(1) Å and 1.63315(1) Å, respectively. The r_e distances of ^{202}HgH$_2$ and ^{202}HgD$_2$ differ by about 0.005%, which can be attributed to the breakdown of the Born−Oppenheimer approximation.

1. Introduction

Mercury and its compounds have been studied extensively as toxic chemicals in the environment.[1−5] Two major anthropogenic sources of mercury in the environment are coal combustion and waste incineration.[1] Mercury in the atmosphere exists mainly as neutral Hg vapor, whereas mercuric salts and methyl−mercury compounds can be found in natural waters and sediments.[4] Anaerobic bacteria in natural waters can reduce Hg(II) to Hg^0, which is re-emitted to the atmosphere as vapor phase elemental mercury.[5,6] The reduction of Hg(II) to Hg^0, followed by the gas-phase detection of atomic mercury, is in fact a well-known method for detecting trace amounts of mercury in liquid and solid samples. The method is called "cold vapor generation", which was developed in the late 1960s, and is based on the reduction of aqueous Hg(II) by SnCl$_2$ or NaBH$_4$ and detection of gas-phase Hg^0 by atomic absorption spectroscopy.[7,8] A similar technique called "hydride generation" is based on the reduction of acidified solutions of group 13, 14, 15, and 16 elements by NaBH$_4$ to form volatile hydrides, which can be detected in the gas phase after atomization.[8] The hydride generation technique was examined recently for mercury, and it was found that both atomic and molecular Hg species are formed in the reduction process.[9] Although this volatile mercury-containing molecule has not been identified, it might be HgH$_2$. In another experiment, methyl-mercury chloride (CH$_3$HgCl) was reduced by NaBH$_4$, and the volatile CH$_3$HgH molecule was detected in the gas phase by FT-IR and mass spectrometry.[10] Considering the fact that anaerobic bacteria can reduce aqueous Hg(II) and aqueous ions of group 14, 15, and 16 elements to form volatile Hg^0, SnH$_4$, PH$_3$, AsH$_3$, and H$_2$S in the environment,[5,6,11,12] a further reduction of Hg^0 by these bacteria may result in formation of volatile HgH$_2$.

There have been several ab initio theoretical studies of the electronic structure and geometry of gaseous HgH$_2$, predicting a linear H−Hg−H structure and a closed-shell $\tilde{X}^1\Sigma_g^+$ ground electronic state.[13−23] The equilibrium Hg−H internuclear distances estimated by various theoretical models were in the range of 1.615−1.713 Å.[13−22] For a heavy atom like Hg, relativistic effects are significant and should be included in the calculations. Nonrelativistic calculations overestimate the Hg−H internuclear distance by more than 0.1 Å.[13−18] Harmonic vibrational frequencies of HgH$_2$, HgHD, and HgD$_2$ have been calculated at the DFT(B3LYP), MP2, and CCSD(T) levels of theory with relatively large basis sets.[19−21] Recently, Li et al.[22] performed a very high level ab initio calculation on this molecule and predicted the energies for many vibrational levels of HgH$_2$, HgHD, and HgD$_2$ for $J = 0$ (no rotation) using a variational calculation. They also calculated that the gas-phase reaction: Hg(g) + H$_2$(g) → HgH$_2$(g) is endoergic by 20.8 kcal mol^{-1} for ground-state (^{1}S) mercury atoms.[22] The first excited state of Hg, the metastable ^{3}P state, lies about 120 kcal mol^{-1} above the ground state,[24] so the formation of gaseous HgH$_2$ from the gas-phase reaction of Hg(^{3}P) with H$_2$ is highly exoergic.

The gas-phase reaction of excited mercury atoms Hg(^{3}P) with molecular hydrogen has been studied by both theoretical calculations and laser pump−probe techniques.[25−32] The ground-state Hg(^{1}S) does not react with H$_2$ because of a high energy barrier, but excited mercury atoms in the ^{3}P state can insert into the H−H bond and form the excited bent [H−Hg−H]* complex.[25−32] This intermediate can dissociate into the HgH and H free radicals. The theoretical and experimental studies of this reaction were focused mainly on the production of HgH and H, and little attention was given to the formation of the ground-state linear H−Hg−H molecule in the gas phase.[28] The reactions of H$_2$ with excited Mg, Zn, Cd, and Hg atoms have been reviewed by Breckenridge.[32]

Solid HgH$_2$ was first synthesized in the 1950s, from the reaction of HgI$_2$ with LiAlH$_4$ in ether-THF-petroleum ether solution at −135 °C.[33−35] This solid was reported to be extremely unstable, decomposing at temperatures above −125 °C,[33−35] and it is probably not possible to produce gaseous HgH$_2$

* Corresponding author. Department of Chemistry, University of Waterloo, 200 University Avenue West, Waterloo, ON, N2L 3G1, Canada. Tel: 519-888-4814. Fax: 519-746-0435. E-mail: bernath@uwaterloo.ca.

by heating the solid. Recently, Wang and Andrews[21,36] recorded the infrared spectra of solid HgH_2, HgHD, and HgD_2 and proposed that HgH_2 forms a covalent molecular solid, unlike zinc and cadmium dihydrides.

Aldridge and Downs[37] have reviewed the chemical properties of group 12 and other main-group hydrides. Many transition-metal hydrides have been trapped in solid matrices at temperatures below 12 K and studied by infrared absorption spectroscopy.[38] Mercury dihydride has been formed in solid hydrogen, nitrogen, neon, and argon matrices from the reaction of excited mercury atoms with hydrogen.[21,36,39,40] The infrared absorption spectra of HgH_2, HgHD, and HgD_2 (trapped in solid matrices) were recorded, and vibrational frequencies of the infrared-active modes were obtained.[21,36,39,40] HgH_2 has also appeared as a byproduct in the matrix isolation experiments designed to study the HHgOH and $Hg(OH)_2$ molecules.[41,42]

We have reported the first observation of HgH_2 and HgD_2 molecules in the gas phase recently.[43] The molecules were generated by the reaction of mercury vapor with molecular hydrogen or deuterium in the presence of an electrical discharge and were identified unambiguously by their high-resolution infrared emission spectra. Rotational analysis of the antisymmetric stretching fundamental bands (ν_3) of HgH_2 and HgD_2 yielded the r_0 Hg−H and Hg−D internuclear distances.[43] Gaseous ZnH_2, ZnD_2, CdH_2, and CdD_2 have also been studied in our laboratory, and detailed analyses of their high-resolution infrared emission spectra have been published.[44−46] A detailed analysis of all of the vibration−rotation bands observed in the infrared emission spectra of gaseous HgH_2 and HgD_2 is presented in this paper.

2. Experimental Section

The emission source used to generate gaseous HgH_2 and HgD_2 molecules has been described in our earlier paper.[43] A small zirconia boat containing about 100 g of mercury was placed inside the central part of an alumina tube. The tube contained stainless steel electrodes in both ends and was sealed with barium fluoride windows. Pure hydrogen or deuterium flowed slowly through the tube at room temperature, and the total pressure was held at 0.7 Torr using a rotary pump. A dc discharge (3 kV/333 mA) was created between the electrodes, and the resulting emission was focused onto the entrance aperture of a Bruker IFS 120 HR Fourier transform spectrometer using a barium fluoride lens. The infrared emission spectrum of HgH_2 was recorded using a KBr beam splitter and an InSb detector cooled by liquid nitrogen. The spectral range was limited to $1750-2200$ cm^{-1} by the detector response and a 2200 cm^{-1} long-wave pass filter. The instrumental resolution was set to 0.01 cm^{-1} and, to improve the signal-to-noise ratio, 100 spectra were co-added during 90 min of recording. The spectrum of HgD_2 was recorded using the same beam splitter and a liquid-nitrogen-cooled HgCdTe (MCT) detector. The spectral range for HgD_2 was $1200-2200$ cm^{-1}, set by the transmission of the 2200 cm^{-1} long-wave pass filter. The instrumental resolution was 0.01 cm^{-1}, and 400 spectra were co-added during 6 h of recording. The signal-to-noise ratios for the strongest emission lines of HgH_2 and HgD_2 were about 100 and 40, respectively.

3. Results and Analysis

3.1. Vibration−Rotation Bands. The WSPECTRA program, written by M. Carleer (Université Libre de Bruxelles), was used to measure the line positions in HgH_2 and HgD_2 spectra. Emission lines of carbon monoxide (impurity) appeared in both
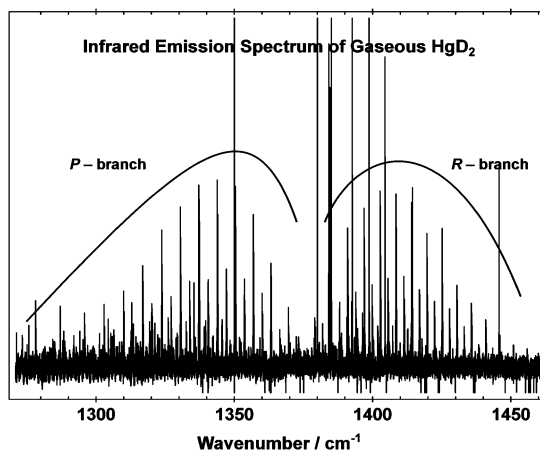

Figure 1. Overview of the infrared emission spectrum of gaseous HgD_2 in the ν_3 region, recorded at a resolution of 0.01 cm^{-1}.
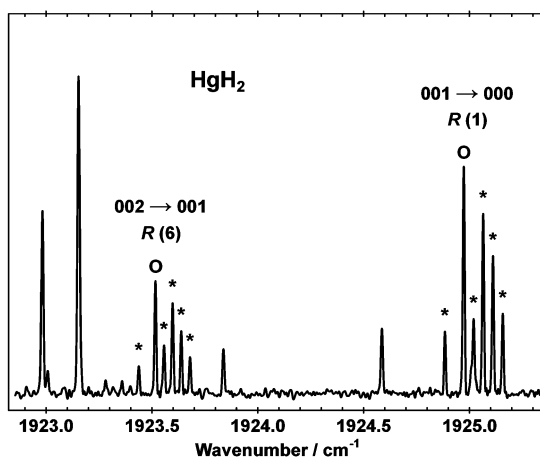

Figure 2. Very small portion of the HgH_2 spectrum showing the isotope splitting in two R-branch lines of the $001 \rightarrow 000$ and $002 \rightarrow 001$ vibration−rotation bands. The lines marked with circles are from $^{202}HgH_2$ and those marked with stars are from minor isotopes of mercury. The strong lines with no isotope splitting are from impurity CO.

spectra and were used for absolute wavenumber calibration.[47] The absolute accuracy of our calibrated line positions is better than 0.0005 cm^{-1}. Rotational assignments of the vibration−rotation bands of HgH_2 and HgD_2 were facilitated using a color Loomis−Wood program.

An overview of the HgH_2 spectrum is shown in Figure 1. Mercury has seven stable isotopes, and their terrestrial abundances are the following: ^{204}Hg (6.9%), ^{202}Hg (29.8%), ^{201}Hg (13.2%), ^{200}Hg (23.1%), ^{199}Hg (16.9%), ^{198}Hg (10.0%), and ^{196}Hg (0.1%). Lines from six isotopes (all except ^{196}Hg) were observed in both spectra, and their intensity ratios match their natural abundances. Figure 2 is a very small portion of the HgH_2 spectrum, showing the isotope splitting in two rotational lines. The adjacent rotational lines in HgH_2 and HgD_2 spectra had 3:1 and 1:2 intensity ratios, respectively, because of the ortho-para nuclear spin statistical weights associated with hydrogen ($I = 1/2$) and deuterium ($I = 1$) nuclei.[48] An expanded view of the HgD_2 spectrum in Figure 3 shows the 1:2 intensity alternation. In addition to the ν_3 fundamental band, that is, 001 (Σ_u^+) → 000 (Σ_g^+), the following hot bands were observed for $^{202}HgH_2$, $^{200}HgH_2$, $^{202}HgD_2$, and $^{200}HgD_2$: 002 (Σ_g^+) → 001 (Σ_u^+), 003 (Σ_u^+) → 002 (Σ_g^+), 101 (Σ_u^+) → 100 (Σ_g^+), and 01^11 (Π_g) → 01^10 (Π_u). Fewer hot bands were detectable for the other isotopes of mercury because of their lower abundances.
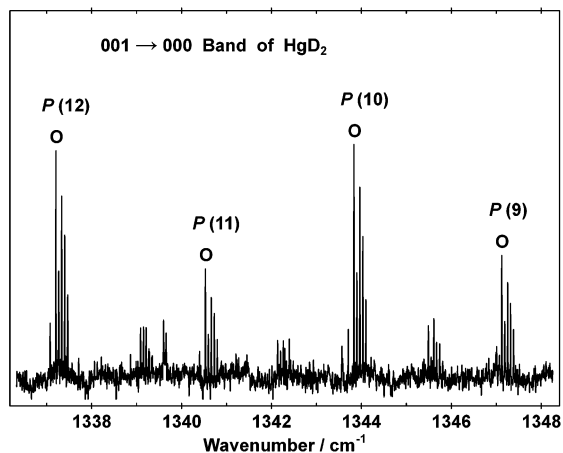
Figure 3. Expanded view of the HgD_2 spectrum showing the 1:2 intensity alternation and the mercury isotope splitting in P-branch lines of the ν_3 fundamental band. The weaker lines are from the hot bands of HgD_2.

The vibrational energy of a linear triatomic molecule in the $^1\Sigma_g^+$ ground electronic state can be expressed by the following equation[48]

$$G(v_1, v_2^l, v_3) = \omega_1(v_1 + (1/2)) + \omega_2(v_2 + 1) + \\ \omega_3(v_3 + (1/2)) + x_{11}(v_1 + (1/2))^2 + x_{22}(v_2 + 1)^2 + \\ x_{33}(v_3 + (1/2))^2 + g_{22}l^2 + x_{12}(v_1 + (1/2))(v_2 + 1) + \\ x_{13}(v_1 + (1/2))(v_3 + (1/2)) + x_{23}(v_2 + 1)(v_3 + (1/2)) \quad (1)$$

in which ω_i values are the harmonic vibrational frequencies and x_{ij} values are second-order anharmonicity constants. The vibrational quantum numbers for the symmetric stretching (σ_g), bending (π_u), and antisymmetric stretching (σ_u) modes are represented by v_1, v_2, and v_3, respectively, and l is the vibrational angular momentum quantum number. The rotational energy for the Σ ($l = 0$) and Π ($l = 1$) states can be expressed by the following equation[49]

$$F_{[v]}(J) = B[J(J + 1) - l^2] - D[J(J + 1) - l^2]^2 \pm \\ \frac{1}{2}[qJ(J + 1) + q_D l^2(J + 1)^2] \quad (2)$$

in which J is the total angular momentum quantum number (including rotation), B is the inertial rotational constant, and D is the centrifugal distortion constant. The rotational l-type doubling parameters, q and q_D, are nonzero only for the Π states, and the $+$ ($-$) sign refers to the e (f) parity component.[48] An experimental uncertainty of 0.0005 cm^{-1} was used for the rotational lines of the $001 \rightarrow 000$ fundamental band of HgH_2 and HgD_2. Lines from the hot bands were less intense and were given an uncertainty of 0.001 cm^{-1}.

The absolute rotational assignments of the 001 (Σ_u^+) $\rightarrow 000$ (Σ_g^+) fundamental bands of HgH_2 and HgD_2 were obtained easily because we observed all of the rotational lines near the band origins. The intensity ratios of adjacent rotational lines further confirmed our absolute J assignments. The rotational assignment of the 002 (Σ_g^+) $\rightarrow 001$ (Σ_u^+) and 003 (Σ_u^+) $\rightarrow 002$ (Σ_g^+) hot bands were obtained consecutively using lower state combination differences. All of the rotational lines of the 001 (Σ_u^+) $\rightarrow 000$ (Σ_g^+), 002 (Σ_g^+) $\rightarrow 001$ (Σ_u^+), and 003 (Σ_u^+) $\rightarrow 002$ (Σ_g^+) bands were fitted together using the energy expression in eq 2, and the spectroscopic constants were determined. A

complete list of the observed line positions for all isotopologues and the outputs of our least-squares fitting program have been placed in Tables 1S–12S, provided as Supporting Information. The spectroscopic constants for $^{202}HgH_2$, $^{200}HgH_2$, $^{202}HgD_2$, and $^{200}HgD_2$ are presented in Tables 1 and 2, and those for the minor isotopes of mercury are in Tables 5S–12S. The ground-state vibrational energy (G_{000}) was set to zero in the least-squares fitting, and the reported constants can reproduce the data within the experimental uncertainty ($\sim$0.001 cm^{-1}).

One of the hot bands in both HgH_2 and HgD_2 spectra had large l-type doubling, and was assigned to the 01^11 (Π_g) $\rightarrow$ 01^10 (Π_u) transition. The absolute J assignment for this band was obtained based on the intensity alternation and the fact that e and f parity components of a Π state have the same vibrational band origins. Rotational lines of the 01^11 (Π_g) $\rightarrow 01^10$ (Π_u) bands of HgH_2 and HgD_2 were fitted using the energy expression in eq 2 with $l = 1$. The vibrational energy of the 01^10 state was set to zero because we can only determine the difference between the 01^11 and 01^10 vibrational energies using our data. Rotational constants and the l-type doubling constants of the 01^10 and 01^11 states are reported in Tables 1 and 2 for $^{202}HgH_2$, $^{200}HgH_2$, $^{202}HgD_2$, and $^{200}HgD_2$.

The absolute J assignments of the 101 (Σ_u^+) $\rightarrow 100$ (Σ_g^+) hot bands of HgH_2 and HgD_2 were difficult to obtain because a few rotational lines near the band origins were missing. Therefore, we had to estimate the rotational constants (B) of the 100 (Σ_g^+) states of HgH_2 and HgD_2 to obtain definite J assignments for these bands. Rotational constants (B) of the 000, 01^10, and 001 states were used to calculate the vibration–rotation interaction constants, α_2 and α_3, for $^{202}HgH_2$ and $^{202}HgD_2$ using the following linear equation:[48]

$$B_{[v]} = B_e - \alpha_1(v_1 + (1/2)) - \alpha_2(v_2 + 1) - \alpha_3(v_3 + (1/2)) \quad (3)$$

Within the Born–Oppenheimer approximation, the ratio of the B_e values of $^{202}HgH_2$ and $^{202}HgD_2$ is simply given by

$$\frac{B_e(^{202}HgH_2)}{B_e(^{202}HgD_2)} = \frac{m_D}{m_H} \quad (4)$$

in which m_D and m_H are atomic masses of deuterium and hydrogen, respectively. In addition, a simple mass-scaling ratio exists for the α_1 constants of $^{202}HgH_2$ and $^{202}HgD_2$:[46,49]

$$\frac{\alpha_1(^{202}HgH_2)}{\alpha_1(^{202}HgD_2)} = \left(\frac{m_D}{m_H}\right)^{3/2} \quad (5)$$

Using the B_{000}, α_2, and α_3 constants of both $^{202}HgH_2$ and $^{202}HgD_2$, we were able to estimate α_1 and B_e for these isotopologues by taking advantage of their isotopic ratios, eqs 3–5. The absolute J assignments of the 101 (Σ_u^+) $\rightarrow 100$ (Σ_g^+) hot bands of HgH_2 and HgD_2 were then obtained immediately because we had reasonable estimates for the α_1 constants. Rotational lines of the 101 (Σ_u^+) $\rightarrow 100$ (Σ_g^+) hot bands were fitted using the energy expression in eq 2 with $l = 0$, and the unknown vibrational energy of the lower state (100, Σ_g^+) was set to zero in the least-squares fitting (see Tables 1 and 2).

In our previous studies on CdH_2 and ZnH_2, we observed local perturbations and Fermi resonance in some vibrational levels.[45,46] The 001 vibrational levels of CdH_2 and ZnH_2 were perturbed locally by the nearby 030 levels because $\nu_3 \approx 3\nu_2$ for these molecules. Strong Fermi resonances were also observed between the 002 (Σ_g^+) and 200 (Σ_g^+) levels because $\nu_3 \approx \nu_1$ for both

TABLE 1: Spectroscopic Constants (in cm^{-1}) of ^{202}HgH$_2$ and ^{200}HgH$_2$

molecule	state	$G_{[v]} - G_{000}$	B	$D/10^{-5}$	$q/10^{-2}$	$q_D/10^{-6}$
^{202}HgH$_2$	000 (Σ_g^+)	0.0	3.0848585(37)[a]	2.83129(76)		
	001 (Σ_u^+)	1912.81427(6)	3.0550309(34)	2.85675(63)		
	002 (Σ_g^+)	3795.38853(17)	3.0231248(40)	2.90922(94)		
	003 (Σ_u^+)	5637.39817(27)	2.9851048(58)	3.0813(19)		
	100 (Σ_g^+)[b]	ν_1	3.036964(32)	2.877(24)		
	101 (Σ_u^+)	1842.02415(30) + ν_1	3.006489(32)	2.902(21)		
	01^{1}0 (Π_u)[b]	ν_2	3.073253(13)	2.8634(53)	−4.3421(18)	1.56(8)
	01^{1}1 (Π_g)	1896.67557(16) + ν_2	3.043677(12)	2.8879(44)	−4.2410(17)	1.44(7)
^{200}HgH$_2$	000 (Σ_g^+)	0.0	3.0848578(39)	2.83101(92)		
	001 (Σ_u^+)	1912.90555(6)	3.0550265(36)	2.85688(78)		
	002 (Σ_g^+)	3795.56107(16)	3.0231103(41)	2.90782(98)		
	003 (Σ_u^+)	5637.62326(24)	2.9850824(55)	3.0864(19)		
	100 (Σ_g^+)[b]	ν_1	3.036962(67)	2.877(65)		
	101 (Σ_u^+)	1842.11402(53) + ν_1	3.006467(68)	2.896(55)		
	01^{1}0 (Π_u)[b]	ν_2	3.073263(18)	2.8634(88)	−4.3412(25)	1.46(14)
	01^{1}1 (Π_g)	1896.76451(22) + ν_2	3.043689(16)	2.8916(69)	−4.2402(23)	1.36(11)

[a] The numbers in parentheses are one standard deviation statistical uncertainties in the last quoted digits. [b] The wavenumbers of ν_1 and ν_2 could not be determined from our data. The best ab initio value (ref 22) for ν_1 is 1982 cm^{-1}, and the neon matrix value (ref 21) for ν_2 is 782 cm^{-1}.

TABLE 2: Spectroscopic Constants (in cm^{-1}) of ^{202}HgD$_2$ and ^{200}HgD$_2$

molecule	state	$G_{[v]} - G_{000}$	B	$D/10^{-5}$	$q/10^{-2}$
^{202}HgD$_2$	000 (Σ_g^+)	0.0	1.5511565(26)[a]	0.70542(24)	
	001 (Σ_u^+)	1375.78848(8)	1.5405124(26)	0.70959(25)	
	002 (Σ_g^+)	2736.90048(20)	1.5294338(30)	0.71714(36)	
	003 (Σ_u^+)	4080.50260(52)	1.5173166(77)	0.7377(21)	
	100 (Σ_g^+)[b]	ν_1	1.534289(21)	0.7105(51)	
	101 (Σ_u^+)	1340.11730(35) + ν_1	1.523499(22)	0.7160(54)	
	01^{1}0 (Π_u)[b]	ν_2	1.547031(10)	0.7126(20)	−1.52172(74)
	01^{1}1 (Π_g)	1367.58606(21) + ν_2	1.536456(10)	0.7188(23)	−1.49770(78)
^{200}HgD$_2$	000 (Σ_g^+)	0.0	1.5511599(31)	0.70558(31)	
	001 (Σ_u^+)	1375.91976(9)	1.5405104(31)	0.70937(31)	
	002 (Σ_g^+)	2737.15442(23)	1.5294221(36)	0.71603(45)	
	003 (Σ_u^+)	4080.85692(59)	1.5172882(90)	0.7297(24)	
	100 (Σ_g^+)[b]	ν_1	1.534306(21)	0.7108(44)	
	101 (Σ_u^+)	1340.24600(38) + ν_1	1.523516(21)	0.7187(42)	
	01^{1}0 (Π_u)[b]	ν_2	1.547042(13)	0.7130(28)	−1.52157(86)
	01^{1}1 (Π_g)	1367.71516(25) + ν_2	1.536455(14)	0.7167(34)	−1.49735(89)

[a] The numbers in parentheses are one standard deviation statistical uncertainties in the last quoted digits. [b] The wavenumbers of ν_1 and ν_2 could not be determined from our data. The best ab initio value (ref 22) for ν_1 is 1421 cm^{-1}, and the neon matrix value (ref 21) for ν_2 is 562 cm^{-1}.

CdH$_2$ and ZnH$_2$.[45,46] In contrast, we did not observe similar perturbations in the vibration−rotation bands of HgH$_2$ and HgD$_2$. Based on the harmonic vibrational frequencies predicted by Greene et al.,[20] ν_1 and $3\nu_2$ are considerably larger than ν_3 for HgH$_2$ and HgD$_2$, and the above perturbations are not expected.

3.2. Determination of Internuclear Distances. The B_{000} constants of ^{202}HgH$_2$, ^{200}HgH$_2$, ^{202}HgD$_2$, and ^{200}HgD$_2$, taken from Tables 1 and 2, were used to determine the r_0 internuclear distances directly from the moment of inertia equation. The r_0 values obtained for ^{202}HgH$_2$ and ^{202}HgD$_2$ are 1.646543(1) Å and 1.642535(2) Å, respectively. This discrepancy (∼0.004 Å) is due to the fact that the 000 ground state of HgD$_2$ lies lower than that of HgH$_2$ on the potential energy surface. However, the r_0 distances for different isotopes of mercury are equal within the statistical uncertainties.

By taking the differences between the ground-state rotational constant (B_{000}) and the $B_{[v]}$ values of the 100, 01^{1}0, and 001

states, we determined the vibration−rotation interaction constants (α_1, α_2, and α_3 in eq 3). The equilibrium rotational constants (B_e) of ^{202}HgH$_2$, ^{200}HgH$_2$, ^{202}HgD$_2$, and ^{200}HgD$_2$ were then calculated using their B_{000} values and the three α's. The equilibrium centrifugal distortion constant (D_e) was calculated for these isotopologues using a linear equation analogous to eq 3 for the $D_{[v]}$ values. Table 3 has a list of molecular constants determined for ^{202}HgH$_2$, ^{200}HgH$_2$, ^{202}HgD$_2$, and ^{200}HgD$_2$ in this study. Using the B_e values of 3.135325(24) cm^{-1} and 1.569037(16) cm^{-1} for ^{202}HgH$_2$ and ^{202}HgD$_2$, respectively, we determined the equilibrium internuclear distances (r_e) to be 1.63324(1) Å and 1.63315(1) Å, respectively. The difference in the r_e values of ^{202}HgH$_2$ and ^{202}HgD$_2$ is only 0.005% but still an order of magnitude larger than the statistical uncertainties. This discrepancy appears to be due to the breakdown of the Born−Oppenheimer approximation.[46] In contrast, the r_e distances for different isotopes of mercury are equal within the statistical uncertainties (see Table 3).

TABLE 3: Molecular Constants (in cm^{-1}) of ^{202}HgH$_2$, ^{200}HgH$_2$, ^{202}HgD$_2$, and ^{200}HgD$_2$

constant	^{202}HgH$_2$	^{200}HgH$_2$	^{202}HgD$_2$	^{200}HgD$_2$
B_{000}	3.084859(4)	3.084858(4)	1.551156(3)	1.551160(3)
r_0/Å	1.646543(1)^a	1.646543(1)	1.642535(2)	1.642534(2)
α_1	0.04789(3)	0.04790(7)	0.01687(2)	0.01685(2)
α_2	0.01161(1)	0.01160(2)	0.00412(1)	0.00412(1)
α_3	0.029828(5)	0.029831(5)	0.010644(4)	0.010649(4)
B_e	3.135325(24)	3.135316(40)	1.569037(16)	1.569029(19)
r_e/Å	1.63324(1)	1.63324(1)	1.63315(1)	1.63315(1)
$D_e/10^{-5}$	2.76(1)	2.76(3)	0.694(3)	0.694(4)
$q_{010}/10^{-2}$	−4.342(2)	−4.341(3)	−1.5217(7)	−1.5216(9)
ν_3	1912.81427(6)	1912.90555(6)	1375.78848(8)	1375.91976(9)
x_{13}	−70.7901(3)	−70.7915(5)	−35.6712(4)	−35.6738(4)
x_{23}	−16.1387(2)	−16.1410(2)	−8.2024(2)	−8.2046(3)
x_{33}	−15.1200(1)	−15.1250(1)	−7.3382(2)	−7.3425(2)
ω_1 (σ_g)	2112^b	2112^b	1492^b	1492^b
ω_2 (π_u)	770^c	774^c		
ω_3 (σ_u)	1994.5880(4)	1994.6924(5)	1416.5030(5)	1416.6463(6)

^{a} The numbers in parentheses are one standard deviation statistical uncertainties, calculated by propagation of errors. ^{b} Estimated from B_e and D_e using eq 8. ^{c} Estimated from q_{010}, B_e and ω_3 using eq 9; the neon matrix values (ref 21) for ν_2 of HgH$_2$ and HgD$_2$ are 782 cm^{-1} and 562 cm^{-1}, respectively.

In polyatomic molecules for which equilibrium internuclear distances (r_e) are not available, it is common to calculate the average r_s structure by using the moments of inertia of isotopically substituted molecules. In our previous work on ZnH$_2$ and ZnD$_2$, we calculated the average r_s structure in order to compare it with the r_0 and r_e internuclear distances.[46] The ground-state moments of inertia (I_0^D and I_0^H) were calculated from the B_{000} values of ^{202}HgD$_2$ and ^{202}HgH$_2$, respectively, and were used to obtain the average r_s distance by the following equation[50] in which m_D and m_H are the atomic masses for deuterium and hydrogen:

$$I_0^D - I_0^H = 2r_s^2(m_D - m_H) \qquad (6)$$

The r_s distance estimated from eq 6 is 1.63851 Å, and lies between the r_0 and r_e values.

3.3. Vibrational Analysis. A few anharmonicity constants in eq 1 can be calculated directly from the observed band origins (Tables 1 and 2). For ^{202}HgH$_2$, ^{200}HgH$_2$, ^{202}HgD$_2$, and ^{200}HgD$_2$ isotopologues, we obtained x_{13} by taking the difference between the $101 \rightarrow 100$ and $001 \rightarrow 000$ band origins. Similarly, the difference between the $01^11 \rightarrow 01^10$ and $001 \rightarrow 000$ band origins is equal to x_{23}, and the difference between the $002 \rightarrow 001$ and $001 \rightarrow 000$ band origins is equal to $2x_{33}$ (see eq 1). All of the hot bands of HgH$_2$ and HgD$_2$ appeared to lower wavenumbers compared to the ν_3 fundamental bands, and thus the x_{13}, x_{23}, and x_{33} constants have negative values (see Table 3). The equilibrium vibrational wavenumber of the antisymmetric stretching mode (ω_3) was then determined using the following equation

$$\nu_3(\text{obs}) = G_{001} - G_{000} = \omega_3 + (1/2)x_{13} + x_{23} + 2x_{33} \qquad (7)$$

which is derived from eq 1.

The equilibrium vibrational wavenumber of the symmetric stretching mode (ω_1) was estimated for ^{202}HgH$_2$, ^{200}HgH$_2$, ^{202}HgD$_2$, and ^{200}HgD$_2$ isotopologues from B_e and D_e constants, using Kratzer's equation for symmetric linear triatomic molecules:[49]

$$D_e \approx \frac{4B_e^3}{\omega_1^2} \qquad (8)$$

The magnitude of the l-type doubling constant (q) depends on B_e, ω_2, and ω_3, and the following third-order equation can be used to estimate the ω_2 constant:[51]

$$q_{010} \approx \frac{-2B_e^2}{\omega_2}\left(1 + \frac{4\omega_2^2}{\omega_3^2 - \omega_2^2}\right) \qquad (9)$$

For ^{202}HgH$_2$ and ^{200}HgH$_2$, we solved eq 9 for ω_2 using our q_{010}, B_e and ω_3 values from Table 3. We were unable to determine the ω_2 constants of ^{202}HgD$_2$ and ^{200}HgD$_2$ from eq 9 because the third-order equation for ω_2 did not have a solution. However, when we used the neon matrix value of 562 cm^{-1} for ν_2 of ^{202}HgD$_2$ in eq 9, along with our B_e and ω_3 values, the predicted q_{010} constant turned out to be −0.01531 cm^{-1}, which differs by less than 1% from the observed value of −0.015217(7) cm^{-1}. It should be noted that eqs 8 and 9 are only approximately correct, and the values of ω_1 and ω_2 obtained from these equations (Table 3) have more than 1% uncertainties.

The absolute vibrational energies of the 100 (Σ_g^+) and 01^10 (Π_u) states, that is, ν_1 and ν_2, could not be determined from our data. The best ab initio values for ν_1 of HgH$_2$ and HgD$_2$ are 1982 cm^{-1} and 1421 cm^{-1}, respectively.[22] The neon matrix values for ν_2 of HgH$_2$ and HgD$_2$ are 782 cm^{-1} and 562 cm^{-1}, respectively.[21]

4. Discussion

4.1. Isotope Effects. The vibrational frequencies for different isotopologues of HgH$_2$ are related by the following equations:[49]

$$\left(\frac{\omega_1^i}{\omega_1}\right)^2 = \left(\frac{m_H}{m_H^i}\right) \qquad (10)$$

$$\left(\frac{\omega_2^i}{\omega_2}\right)^2 = \left(\frac{\omega_3^i}{\omega_3}\right)^2 = \left(\frac{m_H}{m_H^i}\right)\left(\frac{m_{Hg}}{m_{Hg}^i}\right)\left(\frac{M^i}{M}\right) \qquad (11)$$

In the above equations, m_H and m_{Hg} are the atomic masses of hydrogen (or deuterium) and mercury, respectively, and M is the total mass of the molecule. The observed ^{200}Hg:^{202}Hg isotope shift for the ν_3 fundamental band of HgH$_2$ is 0.0913 cm^{-1} and corresponds to a ratio of 1.0000477 between the ν_3 fundamentals of ^{200}HgH$_2$ and ^{202}HgH$_2$. The ratio predicted by eq 11 is 1.0000495. Similarly, the observed ^{200}Hg:^{202}Hg isotope shift for the ν_3 fundamental band of HgD$_2$ is 0.1313 cm^{-1}, corresponding

TABLE 4: Vibrational Wavenumbers and Metal−Hydrogen Internuclear Distances of ZnH$_2$, ZnD$_2$, CdH$_2$, CdD$_2$, HgH$_2$, and HgD$_2$

molecule	$\nu_3 (\sigma_u)$/cm^{-1} gas phase[a]	$\nu_3 (\sigma_u)$/cm^{-1} neon matrix	$\nu_2 (\pi_u)$/cm^{-1} neon matrix	r_0/Å experiment	r_e/Å experiment	r_e/Å ab initio
^{64}ZnH$_2$	1889.4326(2)[b]	1880.6[c]	632.5[c]	1.535274(2)[b]	1.52413(1)[b]	1.527[d]
^{64}ZnD$_2$	1371.6310(2)[b]	1362.6[c]	456.4[c]	1.531846(3)[b]	1.52394(1)[b]	1.527[d]
^{114}CdH$_2$	1771.5296(2)[e]	1764.1[c]	604.0[c]	1.683034(2)[e]		1.668[d]
^{114}CdD$_2$	1278.3117(3)[e]	1271.0[c]	434.5[c]	1.679172(5)[e]		1.668[d]
^{202}HgH$_2$	1912.81427(6)	1918.1[f]	781.7[f]	1.646543(1)	1.63324(1)	1.639[g]
^{202}HgD$_2$	1375.78848(8)	1378.5[f]	561.9[f]	1.642535(2)	1.63315(1)	1.639[g]

[a] The numbers in parentheses are one standard deviation statistical uncertainties. [b] From ref 46. [c] From ref 56. [d] From ref 20. [e] From ref 45. [f] From ref 21. [g] From ref 22; the best ab initio values for the ν_3 of HgH$_2$ and HgD$_2$ (ref 22) are 1885.66 cm^{-1} and 1355.32 cm^{-1}, respectively.

to a ratio of 1.0000954 between the ν_3 fundamentals of ^{200}HgD$_2$ and ^{202}HgD$_2$, whereas a ratio of 1.0000979 is predicted by eq 11. The observed ratio between the ν_3 fundamentals of ^{202}HgH$_2$ and ^{202}HgD$_2$ (Tables 1 and 2) is 1.3903 and the predicted ratio from eq 11 is 1.4067. If we use our ω_3 wavenumbers from Table 3 instead, the agreement becomes better and a ratio of 1.4081 is obtained. The observed H:D isotopic ratio for ω_1 of ^{202}HgH$_2$ and ^{202}HgD$_2$ (Table 3) is 1.4151, and the predicted ratio from eq 10 is 1.4137.

The B_e, α_1, and D_e constants of HgH$_2$ are not sensitive to the mass of mercury, and they should change only when hydrogen is substituted with deuterium.[46] The mass dependences of B_e and α_1 are given in eqs 4 and 5, and the mass dependence of D_e is obtained easily by combining eqs 4, 8, and 10. The observed ratios between the B_e, α_1, and D_e constants of ^{202}HgH$_2$ and ^{202}HgD$_2$ (Table 3) are 1.99825, 2.840, and 3.984, respectively, whereas the predicted ratios are 1.99846, 2.825, and 3.994, respectively. Equations 4, 9, and 11 can be combined to obtain the mass dependence of the *l*-type doubling constant (*q*). The observed ratio between q_{010} constants of ^{202}HgH$_2$ and ^{202}HgD$_2$ is 2.8534 and the predicted ratio is 2.8391. Overall, the observed isotope effects are in good agreement with the theoretical predictions. Within the Born−Oppenheimer approximation, all of the isotopologues should have the same equilibrium internuclear distance (r_e). We found that r_e values (Table 3) are the same for different isotopes of mercury, within their experimental uncertainties. The 0.005% difference between the r_e values of ^{202}HgH$_2$ and ^{202}HgD$_2$ can be attributed to the breakdown of the Born−Oppenheimer approximation.

4.2. Comparison with Theory. A high level ab initio calculation has been performed by Li et al.[22] to obtain the potential energy surface of the $\tilde{X}^1\Sigma_g^+$ ground electronic state of HgH$_2$. They computed the potential energy at 13 000 points using the multireference configuration interaction (MRCI) method with very large basis sets. The potential energy surface was constructed from the ab initio points, and the vibrational energy levels (at $J = 0$) were obtained for HgH$_2$, HgHD, and HgD$_2$ by solving the exact vibration−rotation Schrödinger equation variationally on this surface. The best available theoretical values for the vibrational energy levels of HgH$_2$, HgHD, and HgD$_2$ are thus those obtained by Li and co-workers.[22] However, the ν_3 values predicted for HgH$_2$ and HgD$_2$ in their calculation are 1885.66 cm^{-1} and 1355.32 cm^{-1}, respectively, whereas the observed ν_3 values in ^{202}HgH$_2$ and ^{202}HgD$_2$ in this study are 1912.81427(6) cm^{-1} and 1375.78848(8) cm^{-1}, respectively (Table 3). It is interesting that even at this high level of theory, the ν_3 values of HgH$_2$ and HgD$_2$ are underestimated by about 27 and 20 cm^{-1}, respectively. The equilibrium internuclear distance (r_e) predicted by Li et al. is 1.639 Å,[22] which is larger than our experimental r_e values (Table 3) by about 0.006 Å. Similar ab initio calculations performed by the same group on magnesium dihydride[52] showed somewhat
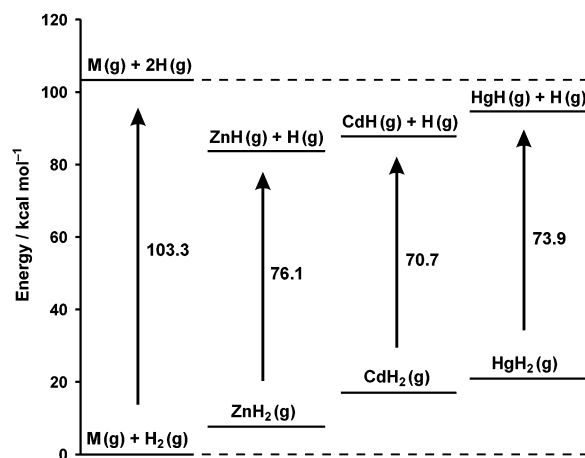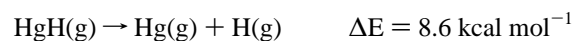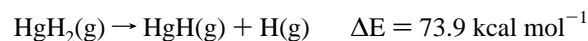

Figure 4. Diagram showing the relative energies of gaseous MH and MH$_2$ molecules (M = Zn, Cd, and Hg). For each metal, the energy of the ground-state M(g) + H$_2$(g) was taken as zero.

better agreement with experiment. The theoretical ν_3 values of MgH$_2$ and MgD$_2$ were smaller than the experimental ones[53,54] by about 13 and 10 cm^{-1}, respectively.

4.3. Comparing HgH$_2$ to ZnH$_2$ and CdH$_2$. The internuclear distances and vibrational wavenumbers of the most abundant isotopologues of ZnH$_2$, ZnD$_2$, CdH$_2$, CdD$_2$, HgH$_2$, and HgD$_2$ are compared in Table 4. The metal−hydrogen internuclear distance in HgH$_2$ is shorter than that of CdH$_2$ because of relativistic effects,[13,18] and the vibrational wavenumbers of HgH$_2$ are larger than those of ZnH$_2$ and CdH$_2$. A combination of experimental and theoretical data can be used to estimate the dissociation energies of the Hg−H bonds in gaseous HgH$_2$. High level ab initio calculations[22] predicted that the gas-phase reaction Hg(g) + H$_2$(g) → HgH$_2$(g) is endoergic by 20.8 kcal mol^{-1} for ground-state mercury atoms. The experimental values for dissociation energies of H$_2$ and HgH are 103.3 and 8.6 kcal mol^{-1}, respectively,[55] and it is straightforward to calculate that the dissociation energy of the first Hg−H bond in HgH$_2$ is 73.9 kcal mol^{-1}, significantly larger than that of the second bond

$$\text{HgH}_2(g) \rightarrow \text{HgH}(g) + \text{H}(g) \qquad \Delta E = 73.9 \text{ kcal mol}^{-1}$$

$$\text{HgH}(g) \rightarrow \text{Hg}(g) + \text{H}(g) \qquad \Delta E = 8.6 \text{ kcal mol}^{-1}$$

Similar patterns exist in the bond energies of gaseous ZnH$_2$ and CdH$_2$, suggesting that average bond strengths should not be used to discuss bonding in these molecules. The best ab initio values for the heats of formation of gaseous ZnH$_2$ and CdH$_2$ from ground-state metal atoms and molecular hydrogen are +7.6 and +17.0 kcal mol^{-1}, respectively,[20] and the experimental values for the dissociation energies of ZnH and CdH are 19.6 and 15.6 kcal mol^{-1}, respectively.[55] Therefore, the dissociation energies of the first metal−hydrogen bond in gaseous ZnH$_2$ and

CdH$_2$ are estimated to be 76.1 and 70.7 kcal mol^{-1}, respectively. The relative energies of gaseous MH and MH$_2$ molecules (M = Zn, Cd, and Hg) are compared in a simple diagram in Figure 4.

5. Conclusions

High-resolution infrared emission spectra of gaseous HgH$_2$ and HgD$_2$ in the ν_3 region were analyzed for six naturally abundant isotopes of mercury. The ν_3 fundamentals of ^{202}HgH$_2$, ^{200}HgH$_2$, ^{202}HgD$_2$, and ^{200}HgD$_2$ were observed at 1912.81427(6), 1912.90555(6), 1375.78848(8), and 1375.91976(9) cm^{-1}, respectively, and the mercury isotope shifts were consistent with the theoretical predictions of eq 11. In addition to the ν_3 fundamental bands of ^{204}HgH$_2$, ^{202}HgH$_2$, ^{201}HgH$_2$, ^{200}HgH$_2$, ^{199}HgH$_2$, ^{198}HgH$_2$, ^{204}HgD$_2$, ^{202}HgD$_2$, ^{201}HgD$_2$, ^{200}HgD$_2$, ^{199}HgD$_2$, and ^{198}HgD$_2$, a few hot bands involving ν_1, ν_2, and ν_3 were assigned and analyzed rotationally to determine spectroscopic constants. Using the rotational constants of the 000, 100, 01^{1}0, and 001 vibrational levels, the equilibrium rotational constants (B_e) of the most abundant isotopologues, ^{202}HgH$_2$ and ^{202}HgD$_2$, were determined to be 3.135325(24) cm^{-1} and 1.569037(16) cm^{-1}, respectively, and the associated equilibrium Hg−H and Hg−D internuclear distances (r_e) are 1.63324(1) Å and 1.63315(1) Å, respectively. The r_e distances of ^{202}HgH$_2$ and ^{202}HgD$_2$ differ by about 0.005%, which can be attributed to the breakdown of the Born−Oppenheimer approximation.

Supporting Information Available: A complete list of the observed line positions and the outputs of least-squares fitting program (Tables 1S−12S). This material is available free of charge via the Internet at http://pubs.acs.org.

References and Notes

(1) Stokstad, E. *Science* **2004**, *303*, 34.
(2) Lu, D. Y.; Granatstein, D. L.; Rose, D. J. *Ind. Eng. Chem. Res.* **2004**, *43*, 5400.
(3) Schroeder, W. H.; Munthe, J. *Atmos. Environ.* **1998**, *32*, 809.
(4) Stein, E. D.; Cohen, Y.; Winer, A. M. *Crit. Rev. Environ. Sci. Technol.* **1996**, *26*, 1.
(5) Mason, R. P.; Morel, F. M. M.; Hemond, H. F. *Water, Air, Soil Pollut.* **1995**, *80*, 775.
(6) Barkay, T.; Miller, S. M.; Summers, A. O. *FEMS Microbiol. Rev.* **2003**, *27*, 355.
(7) Hatch, W. R.; Ott, W. L. *Anal. Chem.* **1968**, *40*, 2085.
(8) Sturgeon, R. E.; Mester, Z. *Appl. Spectrosc.* **2002**, *56*, 202A.
(9) Feng, Y.-L.; Sturgeon, R. E.; Lam, J. W. *Anal. Chem.* **2003**, *75*, 635.
(10) Filippelli, M.; Baldi, F.; Brinckman, F. E.; Olson, G. J. *Environ. Sci. Technol.* **1992**, *26*, 1457.
(11) Weber, J. H. *Mar. Chem.* **1999**, *65*, 67.
(12) Thayer, J. S. *Environmental Chemistry of the Heavy Elements: Hydrido and Organo Compounds*; VCH: New York, 1995.
(13) Pyykkö, P. *J. Chem. Soc., Faraday Trans. 2* **1979**, *75*, 1256.
(14) Dolg, M.; Küchle, W.; Stoll, H.; Preuss, H.; Schwerdtfeger, P. *Mol. Phys.* **1991**, *74*, 1265.
(15) Schwerdtfeger, P.; Heath, G. A.; Dolg, M.; Bennet, M. A. *J. Am. Chem. Soc.* **1992**, *114*, 7518.
(16) Schwerdtfeger, P.; Boyd, P. D. W.; Brienne, S.; McFeaters, J. S.; Dolg, M.; Liao, M.-S.; Schwarz, W. H. E. *Inorg. Chim. Acta* **1993**, *213*, 233.
(17) Kaupp, M.; von Schnering, H. G. *Inorg. Chem.* **1994**, *33*, 2555.
(18) Kaupp, M.; von Schnering, H. G. *Inorg. Chem.* **1994**, *33*, 4179.
(19) Pyykkö, P.; Straka, M.; Patzschke, M. *Chem. Commun.* **2002**, 1728.
(20) Greene, T. M.; Brown, W.; Andrews, L.; Downs, A. J.; Chertihin, G. V.; Runeberg, N.; Pyykkö, P. *J. Phys. Chem.* **1995**, *99*, 7925.
(21) Wang, X.; Andrews, L. *Phys. Chem. Chem. Phys.* **2005**, *7*, 750.
(22) Li, H.; Xie, D.; Guo, H. *J. Chem. Phys.* **2005**, *122*, 144314.
(23) von Szentpály, L. *J. Phys. Chem. A* **2002**, *106*, 11945.
(24) Burns, K.; Adams, K. B.; Longwell, J. *J. Opt. Soc. Am.* **1950**, *40*, 339.
(25) Breckenridge, W. H.; Jouvet, C.; Soep, B. *J. Chem. Phys.* **1986**, *84*, 1443.
(26) Bras, N.; Butaux, J.; Jeannet, J. C.; Perrin, D. *J. Chem. Phys.* **1986**, *85*, 280.
(27) Bernier, A.; Millie, P. *Chem. Phys. Lett.* **1987**, *134*, 245.
(28) Bernier, A.; Millie, P. *J. Chem. Phys.* **1988**, *88*, 4843.
(29) Bras, N.; Jeannet, J. C.; Butaux, J.; Perrin, D. *J. Chem. Phys.* **1991**, *95*, 1006.
(30) Siegbahn, P. E. M.; Svensson, M.; Crabtree, R. H. *J. Am. Chem. Soc.* **1995**, *117*, 6758.
(31) Ohmori, K.; Takahashi, T.; Chiba, H.; Saito, K.; Nakamura, T.; Okunishi, M.; Ueda, K.; Sato, Y. *J. Chem. Phys.* **1996**, *105*, 7464.
(32) Breckenridge, W. H. *J. Phys. Chem.* **1996**, *100*, 14840.
(33) Wiberg, E.; Henle, W. *Z. Naturforsch.* **1951**, *6b*, 461.
(34) Wiberg, E. *Angew. Chem.* **1953**, *65*, 16.
(35) Mueller, W. M.; Blackledge, J. P.; Libowitz, G. G. *Metal Hydrides*; Academic Press: New York, 1968.
(36) Wang, X.; Andrews, L. *Inorg. Chem.* **2004**, *43*, 7146.
(37) Aldridge, S.; Downs, A. J. *Chem. Rev.* **2001**, *101*, 3305.
(38) Andrews, L. *Chem. Soc. Rev.* **2004**, *33*, 123.
(39) Legay-Sommaire, N.; Legay, F. *Chem. Phys. Lett.* **1993**, *207*, 123.
(40) Legay-Sommaire, N.; Legay, F. *J. Phys. Chem.* **1995**, *99*, 16945.
(41) Macrae, V. A.; Greene, T. M.; Downs, A. J. *Phys. Chem. Chem. Phys.* **2004**, *6*, 4586.
(42) Wang, X.; Andrews, L. *Inorg. Chem.* **2005**, *44*, 108.
(43) Shayesteh, A.; Yu, S.; Bernath, P. F. *Chem.−Eur. J.* **2005**, *11*, 4709.
(44) Shayesteh, A.; Appadoo, D. R. T.; Gordon, I. E.; Bernath, P. F. *J. Am. Chem. Soc.* **2004**, *126*, 14356.
(45) Yu, S.; Shayesteh, A.; Bernath, P. F. *J. Chem. Phys.* **2005**, *122*, 194301.
(46) Shayesteh, A.; Gordon, I. E.; Appadoo, D. R. T.; Bernath, P. F. *Phys. Chem. Chem. Phys.* **2005**, *7*, 3132.
(47) Maki, A. G.; Wells, J. S. *Wavenumber Calibration Tables from Heterodyne Frequency Measurements*; NIST Special Publication 821, U.S. Government Printing Office: Washington, DC, 1991.
(48) Bernath, P. F. *Spectra of Atoms and Molecules*, 2nd ed.; Oxford University Press: New York, 2005.
(49) Herzberg, G. *Molecular Spectra and Molecular Structure II. Infrared and Raman Spectra of Polyatomic* Molecules; Krieger: Malabar, FL, 1991.
(50) Chutjian, A. *J. Mol. Spectrosc.* **1964**, *14*, 361.
(51) Watson, J. K. G. *Can. J. Phys.* **2001**, *79*, 521.
(52) Li, H.; Xie, D.; Guo, H. *J. Chem. Phys.* **2004**, *121*, 4156.
(53) Shayesteh, A.; Appadoo, D. R. T.; Gordon, I.; Bernath, P. F. *J. Chem. Phys.* **2003**, *119*, 7785.
(54) Shayesteh, A.; Appadoo, D. R. T.; Gordon, I.; Bernath, P. F. *Can. J. Chem.* **2004**, *82*, 947.
(55) Huber, K. P.; Hezberg, G. *Molecular Spectra and Molecular Structure IV. Constants of Diatomic* Molecules; Van Nostrand: New York, 1979.
(56) Wang, X.; Andrews, L. *J. Phys. Chem. A* **2004**, *108*, 11006.